Resonances and time-delay in three-body scattering

J. P. Svenne and T. A. Osborn
Department of Physics, University of Manitoba, Winnipeg, Manitoba, Canada R3T 2N2

G. Pisent
Dipartimento di Fisica dell'Università Padova, Istituto Nazionale di Fisica Nucleare, Sezione di Padova, Padova, Italy

D. Eyre
Departement Wiskunde en Toegepaste Wiskunde, Potchefstroomse Universiteit vir Christelike Hoër Onderwys, Vanderbijlpark, Republic of South Africa

(Received 17 April 1989)

Time delay and resonant phenomena are examined in the context of a model three-body problem. The time-delay formalism is reviewed and summarized, as it applies to a three-body system. Calculations are carried out for a three-body model containing elastic, inelastic, and rearrangement channels. The two-body interactions in the model permit two-body resonances to be embedded in the three-body structure. Eigenvalues of the time-delay matrix are shown to provide a clear, unambiguous signature of resonant behavior in the multichannel system. A resonance always shows up as a positive peak in *one* eigenvalue of the time-delay matrix. This result is contrasted with the more usual means of identifying resonant behavior by studying the phases of the S-matrix elements, or the eigenphases of the S matrix.

I. INTRODUCTION

This paper investigates time delay and resonant phenomena in the three-body problem. Using a variety of two-body potentials we computationally solve the three-body problem for all incident energies below the breakup threshold. For the family of potentials we employ, this energy range includes elastic, inelastic, and rearrangement scattering processes. Throughout this energy range the full multichannel S matrix is determined and from it the associated time-delay matrix is constructed. We use the time-delay matrix as a descriptive tool in order to infer the presence or absence of resonant behavior in the multichannel scattering sectors.

The time-delay characterization of the collision processes is interesting for several reasons. The first of these is that the time delay provides an extension of the phase-shift concept that remains applicable in complex scattering situations, where phase shifts are not defined by conventional means. This possibility is seen from Wigner's identity[1] that relates the time delay $q(E)$ for a given angular momentum state to the phase shift,

$$q(E)=2\frac{d\delta}{dE} . \tag{1.1}$$

Since δ and q are obtained from each other by an integration or differentiation in the energy variable they contain (modulo an integration constant) the same information. In multichannel scattering or two-body scattering from nonspherically symmetric potentials a single phase-shift decomposition of the scattering process is unavailable. Nevertheless time delay (the operator and its trace) remains well defined, and provides information about the collision process.

The second feature of interest, and one closely related to the principal motivation of this work, is that the definition of the multichannel time-delay operator is based on the idea of some portion of the scattering wave packet being trapped in the coordinate region of the target longer than free evolution would predict. For this reason long time delays are a direct manifestation of resonant behavior.

Numerical calculations of time delay in the few-body multichannel context is a largely unexplored topic. See, however, Kupperman and Kaye[2] for an application to a problem in one dimension in chemistry. A basic difficulty is that one must know the full S matrix for a range of scattering energies. This means that the scattering problem must be solved for all possible open incoming channels. By using finite-rank two-body interactions and an efficient numerical realization of Faddeev's equations these difficulties have been overcome. We have not extended our calculations above the breakup threshold. To do so would require calculating the three-to-three scattering S matrix and at present there is no agreed upon definition of time delay for this channel and the associated renormalizations that are required to make the time-delay finite.

II. TIME-DELAY FORMALISM

Time-delay theory provides a quantitative description of any temporal trapping of a scattering wave packet that is caused by the interaction between a target and an incoming projectile. A balanced overview of the three-body time-delay formalism will emerge if one compares single-channel (or two-body) scattering with the multichannel case. In this brief sketch of the theory we con-

sider only the definitions of time delay and the related predictions that prove useful in interpreting the exact three-body calculations reported in Sec. V.

First consider two-body scattering. After removal of the center-of-mass motion the Hilbert space of quantum states is $\mathcal{H}=L^2(\mathbf{x})$. Here the vector $\mathbf{x}\in\mathbf{R}^3$ denotes vector separation of the two particles and we label the momentum conjugate to $\mathbf{x}$ as $\mathbf{p}$. The pair of interacting and free Hamiltonians, (h,h_0) define a scattering system. Specifically if m is the two-body reduced mass, h_0 is the kinetic energy $\mathbf{p}^2/2m$, and V the operator-valued potential then the full Hamiltonian reads

$$h=h_0+V\ . \tag{2.1}$$

More precisely one has a scattering system if (a) the wave operators exist,

$$\Omega^{(\pm)}=\underset{t\to\mp\infty}{s\text{-lim}}\,[\exp(+iht)\exp(-ih_0t)]\ ; \tag{2.2}$$

(b) asymptotic completeness is valid, i.e., the wave operators $\Omega^{(+)}$ and $\Omega^{(-)}$ have the same range and the orthogonal complement of this range in $L^2(\mathbf{x})$ is spanned by the eigenfunctions of h. Results (a) and (b) are well known if the operator V is defined by multiplication by a local potential function,[3,4] $v(\mathbf{x})\in L^2(\mathbf{x})$, that has for large $\mathbf{x}$ argument an algebraic decay more rapid than $|\mathbf{x}|^{-1}$, or alternately, is a finite-rank separable potential with form factors that decay faster than $|\mathbf{x}|^{-1}$.

In this terminology the conventional S matrix is given by

$$S=\Omega^{(-)\dagger}\Omega^{(+)}\ . \tag{2.3}$$

Asymptotic completeness ensures that S is unitary. Suppose $f_{\text{in}}\in L^2(\mathbf{x})$ is the time-independent characterization of an arbitrary incoming state. Such a state evolves freely from $t=-\infty$ via

$$\Phi_{\text{in}}(t)=\exp(-ih_0t)f_{\text{in}}\ . \tag{2.4}$$

The $+$ labeling of the wave operator $\Omega^{(+)}$ employs the convention that the function $\Phi_{\text{in}}(t)$ is matched [in the $L^2(\mathbf{x})$ norm sense] to the exactly evolving wave function $\Psi(t)$ at $t=-\infty$. Specifically,

$$\Psi(t)=\exp(-iht)\Omega^{(+)}f_{\text{in}}=\Omega^{(+)}\Phi_{\text{in}}(t)\ . \tag{2.5}$$

For a given initial state the associated time delay is the difference of the quantum transit times of $\Psi(t)$ and $\Phi_{\text{in}}(t)$ through a fixed coordinate space region. We take this region to be a sphere about $\mathbf{x}=\mathbf{0}$ of radius r, and denote by P_r the projection operator onto this coordinate region. With these objects one constructs a Hermitian operator Q_r, whose diagonal matrix element is the time delay for region associated with P_r, namely,

$$(f_{\text{in}},Q_rf_{\text{in}})=\int_{-\infty}^{\infty}dt[\|P_r\Psi(t)\|^2-\|P_r\Phi_{\text{in}}(t)\|^2]\ . \tag{2.6a}$$

Or equivalently in terms of the wave operators

$$(f_{\text{in}},Q_rf_{\text{in}})=\int_{-\infty}^{\infty}dt(\Phi_{\text{in}}(t),[\Omega^{(+)\dagger}P_r\Omega^{(+)}-P_r]\Phi_{\text{in}}(t))\ . \tag{2.6b}$$

The operator Q_r shares a number of basic features with the S matrix. For example, both operators commute with h_0,

$$Sh_0=h_0S\ , \tag{2.7a}$$

$$Q_rh_0=h_0Q_r\ . \tag{2.7b}$$

This means that both S and Q_r conserve energy and have similar diagonal energy representations, viz.,

$$\langle\mathbf{p}'|S|\mathbf{p}\rangle=\delta(E'-E)\langle\hat{\mathbf{p}}'|s(E)|\hat{\mathbf{p}}\rangle\ , \tag{2.8a}$$

$$\langle\hat{\mathbf{p}}'|s(E)|\hat{\mathbf{p}}\rangle=\delta(\hat{\mathbf{p}}'-\hat{\mathbf{p}})-2\pi it(\hat{\mathbf{p}}',\hat{\mathbf{p}};E+i0)\ , \tag{2.8b}$$

where the function t denotes the on-energy-shell t matrix that is proportional to the scattering amplitude. The unit-length vectors $\hat{\mathbf{p}}$ and $\hat{\mathbf{p}}'$ denote, respectively, the incident and exit momentum directions. In the expression (2.8b) the matrix element $\langle\hat{\mathbf{p}}'|s(E)|\hat{\mathbf{p}}\rangle$ is the integral kernel for the on-energy-shell operator $s(E)$. This latter operator maps the space $L^2(\hat{\mathbf{p}})$ into $L^2(\hat{\mathbf{p}})$. The energy decomposition of Q_r having the same format as S is

$$\langle\mathbf{p}'|Q_r|\mathbf{p}\rangle=\delta(E'-E)\langle\hat{\mathbf{p}}'|q_r(E)|\hat{\mathbf{p}}\rangle\ . \tag{2.9a}$$

The simple relationship between time delay and the energy-dependent S matrix now takes the form

$$q(E)=-i\hbar s(E)^\dagger\frac{d}{dE}s(E)\ , \tag{2.9b}$$

where $q(E)$ represents the limiting value of $q_r(E)$ as $r\to\infty$.

The remaining property of time delay that is helpful in the interpretation of scattering data is the spectral property. Let $r(z)=(h-z)^{-1}$ and $r_0(z)=(h_0-z)^{-1}$ be the resolvent operators for the Hamiltonians, h and h_0, that are defined for complex energy z. Then the spectral property is the statement that

$$2\,\text{Im}\,\text{Tr}[r(E+i0)-r_0(E+i0)]=\text{tr}q(E),\quad E>0\ . \tag{2.10}$$

In this equation Tr is the trace on the space $L^2(\mathbf{x})$, while tr is the trace on $L^2(\hat{\mathbf{p}})$—i.e., all square integrable functions on the surface of a unit-radius sphere in $\mathbf{R}^3$. The spectral property has a simple physical interpretation. The left-hand side of (2.10) is the change of state density at energy E produced by the perturbing potential V. Thus (2.10) states that the trace of $q(E)$ is proportional to the state density shift induced by V. If there is a large relative increase in the number of states at a particular energy E, then $\text{tr}q(E)$ must be large. It is the spectral property that makes the time delay useful also in deriving generalized Levinson's theorems[5-7] and in finding Laplace transform representations of virial coefficients for a quantum gas.[8-11]

Having described the definition of two-particle time delay, its characterization in terms of the S matrix, and the related spectral property, we must consider these three key features in the context of the three-body scattering. By and large, our notation closely follows that of Faddeev.[12] We use the Jacobi variables $\mathbf{x}_\alpha,\mathbf{y}_\alpha$ to represent the spatial coordinates of the three-body system. These six degrees of freedom completely specify the orientation

of the three particles relative to the three-body center-of-mass position. The variable $\mathbf{x}_\alpha$ is the vector separation of the particle α from the center of mass of the (β,γ) cluster. The remaining independent coordinate $\mathbf{y}_\alpha$ gives the vector separation of the constituents of the α cluster; namely, the spatial separation of particles β and γ. The canonically conjugate momenta related to $\mathbf{x}_\alpha$ and $\mathbf{y}_\alpha$ are denoted by $\mathbf{p}_\alpha$ and $\mathbf{q}_\alpha$. The momentum $\mathbf{p}_\alpha$ specifies the relative motion of particle α and cluster α. Let m_α $(\alpha=1,2,3)$ be the masses of the three particles; then

$$n_\alpha=m_\alpha(m_\beta+m_\gamma)/(m_\alpha+m_\beta+m_\gamma)$$

represents the reduced mass of particle α and cluster α. The kinetic energy of this relative motion is $\mathbf{p}_\alpha^2/2n_\alpha$. The internal momentum of the particles forming cluster α is just $\mathbf{q}_\alpha$. Cluster α has reduced mass

$$\mu_\alpha=m_\beta m_\gamma/(m_\beta+m_\gamma)$$

and an internal kinetic energy $\mathbf{q}_\alpha^2/2\mu_\alpha$. With this notation, the free three-particle kinetic energy Hamiltonian is

$$\begin{aligned}H_0&=\mathbf{p}_\alpha^2/2n_\alpha+\mathbf{q}_\alpha^2/2\mu_\alpha\\&=\mathbf{p}_1^2/2m_1+\mathbf{p}_2^2/2m_2+\mathbf{p}_3^2/2m_3\ .\end{aligned}\tag{2.11}$$

The dynamical motion of the three-particle state is governed by the various Hamiltonians that the system admits. Let V_α denote the potential acting between particles β and γ. Thus we may define the Hamiltonians

$$H_\alpha=H_0+V_\alpha,\quad \alpha=1,2,3\ ,\tag{2.12a}$$

$$H=H_0+\sum_{\alpha>0}V_\alpha\ .\tag{2.12b}$$

These Hamiltonians are linear operators on the Hilbert space $\mathcal{H}=L^2(\mathbf{x}_\alpha,\mathbf{y}_\alpha)$. Since the interactions V_β and V_γ decay for large particle separation, H_α will approximately govern the time evolution of the system if particle α and cluster α are far apart.

Consider the multichannel Møller operators that define the standard two-Hilbert-space scattering theory.[12] As in the two-body problem, these Møller operators are a principal ingredient in the definition of the multichannel time delay. Consider first the two-particle subsystems contained within the three-body problem. The coordinate space kernel representation of V_α suitable for both local and separable interactions is

$$\langle\mathbf{x}_\alpha\mathbf{y}_\alpha|V_\alpha|\mathbf{x}'_\alpha\mathbf{y}'_\alpha\rangle=\delta(\mathbf{x}_\alpha-\mathbf{x}'_\alpha)v_\alpha(\mathbf{y}_\alpha,\mathbf{y}'_\alpha)\ .\tag{2.13}$$

The two-body momentum space potential given in Sec. IV is the Fourier transform of $v_\alpha(\mathbf{y}_\alpha,\mathbf{y}'_\alpha)$. Let h_α be the two-particle Hamiltonian for particles β and γ, and let $\phi_{\alpha i}$ be the ith independent unit-normalized eigenfunction of h_α having binding energy $-\varepsilon_{\alpha i}$

$$h_\alpha\phi_{\alpha i}=(\mathbf{q}_\alpha^2/2\mu_\alpha+v_\alpha)\phi_{\alpha i}=-\varepsilon_{\alpha i}\phi_{\alpha i}\ .\tag{2.14}$$

In the numerical solutions of the scattering problem described in Sec. IV, the maximum value of i is 2. For each stable cluster, there is an associated channel Hilbert space $\mathcal{H}_{\alpha i}=L^2(\mathbf{x}_\alpha)$. The channel identification operator $J_{\alpha i}$ then maps $f_{\alpha i}\in\mathcal{H}_{\alpha i}$ into an element of $\mathcal{H}$ via the definition

$$(J_{\alpha i}f_{\alpha i})(\mathbf{x}_\alpha,\mathbf{y}_\alpha)=\phi_{\alpha i}(\mathbf{y}_\alpha)f_{\alpha i}(\mathbf{x}_\alpha)\ .\tag{2.15}$$

In terms of the $J_{\alpha i}$, the wave operators are given by

$$\Omega_{\alpha i}^{(\pm)}=s\text{-}\lim_{t\to\mp\infty}[\exp(+iHt)\exp(-iH_\alpha t)]J_{\alpha i}\ .\tag{2.16}$$

The operators $\Omega_{\alpha i}^{(+)}$ map functions from an incident channel space $\mathcal{H}_{\alpha i}$ into the full three-body space $\mathcal{H}=L^2(\mathbf{x}_\alpha,\mathbf{y}_\alpha)$. Likewise, $\Omega_{\beta j}^{(-)}$ maps functions from the outgoing channel $\mathcal{H}_{\beta j}$ into $\mathcal{H}$. The wave operator $\Omega_{\alpha i}^{(+)}$ allows one to construct the exact time-dependent solution of the Schrödinger equation, which at time $t=-\infty$ is described by particle α incident on cluster α in an eigenstate $\phi_{\alpha i}$ and having a relative motion wave function $f_{\alpha i}$. [This corresponds, for channel αi, to the function f_{in} of the two-body problem, Eq. (2.4). We drop the designation "in," for simplicity of notation. Likewise, below in Eq. (2.18b), the designation "out" will be dropped, and the function will be denoted simply $f'_{\alpha i}$.] The exact time-evolving wave function is

$$\begin{aligned}\Psi(t)&=\exp(-iHt)\Omega_{\alpha i}^{(+)}f_{\alpha i}\\&=\Omega_{\alpha i}^{(+)}\exp(-i\tilde{H}_{\alpha i}t)f_{\alpha i}\ ,\end{aligned}\tag{2.17}$$

where $\tilde{H}_{\alpha i}$ is the energy operator $\mathbf{p}_\alpha^2/2n_\alpha-\varepsilon_{\alpha i}$ valid for channel αi. In this terminology, the multichannel S matrix maps the incoming channel space $\mathcal{H}_{\alpha i}$ onto the outgoing channel space $\mathcal{H}_{\beta j}$ via

$$S_{\beta j;\alpha i}=\Omega_{\beta j}^{(-)\dagger}\Omega_{\alpha i}^{(+)}\ ,\tag{2.18a}$$

$$f'_{\beta j}=S_{\beta j;\alpha i}f_{\alpha i}\ .\tag{2.18b}$$

The intertwining property

$$S_{\beta j;\alpha i}\tilde{H}_{\alpha i}=\tilde{H}_{\beta j}S_{\beta j;\alpha i}\tag{2.19a}$$

expresses the multichannel form of the energy-conserving property of the S matrix. Like the commutation (2.7a) in the two-body case, identity (2.19a) implies that the momentum matrix elements of the S matrix are diagonal in energy and thereby serves to define a reduced on-energy-shell S-matrix operator mapping $L^2(\hat{\mathbf{p}}_\alpha)$ to $L^2(\hat{\mathbf{p}}_\beta)$; namely,

$$\begin{aligned}\langle\mathbf{p}'_\beta|S_{\beta j;\alpha i}|\mathbf{p}_\alpha\rangle&=\delta(E'_\beta-E_\alpha)(n_\beta p'_\beta n_\alpha p_\alpha)^{-1/2}\\&\times\langle\hat{\mathbf{p}}'_\beta|s_{\beta j;\alpha i}(E)|\hat{\mathbf{p}}_\alpha\rangle\ .\end{aligned}\tag{2.19b}$$

Two basic forms stating the unitarity of the S matrix follow from the notation above—one for the full S matrix, the other for the reduced S matrix. For the full S matrix, we have

$$\delta_{\beta j;\alpha i}=\sum_{\gamma k}S^\dagger_{\gamma k;\beta j}S_{\gamma k;\alpha i}\ ,\tag{2.20a}$$

while in terms of the reduced S matrices, unitarity takes the on-energy-shell form

$$\hat{\delta}_{\beta j;\alpha i}=\sum_{\gamma k}s^\dagger(E)_{\gamma k;\beta j}s(E)_{\gamma k;\alpha i}\ .\tag{2.20b}$$

Here, if $\alpha i=\beta j$, then $\delta_{\beta j;\alpha i}$ is the identity operator in $L^2(\mathbf{p}_\alpha)$, whereas $\hat{\delta}_{\beta j;\alpha i}$ is the identity operator in $L^2(\hat{\mathbf{p}}_\alpha)$.

The multichannel time delay is given in terms of the

difference of sojourn times in a given region of space of the asymptotic and exact wave packets. In the Jacobi variable space, $\mathbf{x}_\alpha, \mathbf{y}_\alpha$, an α-independent radial length is given by

$$\rho^2=(n_\alpha \mathbf{x}_\alpha^2+\mu_\alpha \mathbf{y}_\alpha{}^2)/m_0 \ , \tag{2.21}$$

where

$$m_0^2=(m_1 m_2 m_3/m_1+m_2+m_3) \ .$$

For each $r>0$ define a projection operator in $\mathcal{H}$ by

$$P_r f(\mathbf{x}_\alpha,\mathbf{y}_\alpha)=f(\mathbf{x}_\alpha,\mathbf{y}_\alpha) \quad \text{if } \rho<r$$
$$=0, \quad \text{otherwise} \ . \tag{2.22}$$

For scattering processes initiated by the collision of two fragments, the definition of time delay within the six-dimensional sphere of radius r is given by the following:

$$Q(f_{\alpha i},r)=\int_{-\infty}^{\infty} dt \left[\|P_r \psi(t)\|^2 - \tfrac{1}{2}\left[\|P_r e^{-iH_\alpha t} J_{\alpha i} f_{\alpha i}\|^2 + \sum_{\beta j} \|P_r e^{-iH_\beta t} J_{\beta j} f'_{\beta j}\|^2 \right] \right] . \tag{2.23}$$

Evaluating the time integral provides an expression for the on-energy-shell form of the time-delay operator $q_{\alpha i}(E,r)$,

$$Q(f_{\alpha i},r)=\int d\mathbf{p}_\alpha d\mathbf{p}'_\alpha \delta(E_{\alpha i}-E'_{\alpha i})[f_{\alpha i}(\mathbf{p}'_\alpha)]^* \times (n_\alpha p_\alpha)^{-1} \langle \mathbf{p}'_\alpha | q_{\alpha i}(E,r) | \mathbf{p}_\alpha \rangle f_{\alpha i}(\mathbf{p}_\alpha) \ . \tag{2.24}$$

Here $E_{\alpha i}=\mathbf{p}_\alpha^2/2n_\alpha-\varepsilon_{\alpha i}$ is the energy in channel αi. In the limit $r\to\infty$, the on-shell time delay operator takes the S-matrix form

$$q_{\alpha i;\alpha i}(E)=\lim_{r\to\infty} q_{\alpha i}(E,r) \ , \tag{2.25}$$

where (2.25) is the elastic channel restriction of the operator

$$q_{\alpha i;\beta j}(E)=-i\sum_{\gamma k} s^\dagger(E)_{\gamma k;\alpha i}\frac{d}{dE}s(E)_{\gamma k;\beta j} \ . \tag{2.26}$$

The formula for $q_{\alpha i;\beta j}(E)$ is given as a matrix of on-energy-shell operators in the channel indices αi and βj. However, as the result (2.23)–(2.24) indicates, it is only the diagonal channel entries that carry the physical significance of time delay.

The time integral (2.23) constructing $Q(f_{\alpha i},r)$ is seen to involve the transit time of the exact wave packet $\Psi(t)$, minus the symmetric average of the traverse times of the free incoming asymptotic wave, plus the traverse times of all the outgoing asymptotic components of the scattering process. If only one channel is open, these incoming and outgoing free traverse times can be shown to be identical. In this latter case, the definition of time delay is parallel to the two-body case. The precise form of the right-hand integral in (2.23) is required if one is to obtain a finite result for $Q(f_{\alpha i},r)$ as $r\to\infty$.

Finally, we state the form that the spectral property assumes. For complex energy z, define the resolvents

$$R(z)=(H-z)^{-1} \ , \tag{2.27a}$$

$$R_\alpha(z)=(H_\alpha-z)^{-1}, \quad \alpha=0,1,2,3 \ . \tag{2.27b}$$

As in the theory of virial coefficients,[10] define the connected resolvent difference by

$$R_C(z)=R(z)-R_0(z)-\sum_{\alpha>0}[R_\alpha(z)-R_0(z)] \ . \tag{2.27c}$$

Then the spectral property is

$$2\,\mathrm{Tr}\,\mathrm{Im}R_C(E+i0)=\sum_{\alpha i}\mathrm{tr}q_{\alpha i;\alpha i}(E) \ . \tag{2.28}$$

The two traces above are those compatible with the operators on which they act. In the three-body Hilbert space $\mathcal{H}$, the trace is denoted Tr and in the on-shell reduced channel space $L^2(\hat{\mathbf{p}}_\alpha)$, the trace is indicated by tr.

The left-hand side of (2.28) is twice the change of the connected state density at energy E, which is induced by the interactions V_α. The right-hand side of (2.28) is the sum of all the traces of the time-delay operators over all open channels αi. If E is below the threshold $-\varepsilon_{\alpha i}$ for channel αi, then $q_{\alpha i;\alpha i}(E)$ is identically zero. The correct statement of the three-body spectral property critically depends on the use of the connected resolvent difference. If one attempted to use just $R(z)-R_0(z)$, then its trace would be divergent. Only the connected resolvent difference has finite trace.

The first heuristic statement of result (2.26) is found in the work of Smith.[13] Demonstration of the time-delay formula (2.26) based upon Faddeev's account of the three-body problem occurs in Refs. 14 and 15. The multichannel spectral property can be found in Refs. 10, 15, and 16. The review by Martin[17] gives a balanced overview of the time-delay formalism.

III. THREE-BODY MODEL

The three-body model used in the calculations in this paper is an extension of the one used in Ref. 18. We consider three particles, labeled 1, 2, and 3. They are spinless equal-mass particles, with 2 and 3 being identical, 1 distinguishable. They interact via two-term finite-rank two-body S-wave interactions. Subsystem (23) supports two bounds states $(1m)$ and $(1n)$, respectively, $(1m)$ being the ground state of the system. The (13) and (12) subsystems interact via identical two-term separable potentials of the form found in Ref. 19. This potential supports one bound state. The realization of this bound state in the (13) subsystem we label $(2s)$ and the bound state found in (12) is called $(3s)$.

The system thus has three channels below the breakup threshold: The elastic channel, an inelastic channel, and a rearrangement channel. (We do not go above the three-body breakup threshold in this work.) The location of the thresholds where the inelastic and rearrangement channels open up can be adjusted at will by varying the parameters of the interactions. The resonance is always

in the (13) or (12) subsystems, but its location relative to the thresholds can also be adjusted, so that its effect can be observed in any energy sector.

The equations of the three-body problem are cast in form which is a generalization of the Amado-Lovelace[20] form of equations, and are solved by a computer code which is an extension of the code used in Ref. 18, to check against the EPR solutions of that work. The schematic structure of these equations is as follows: The (23) subsystem amplitudes are obtained from

$$X_{\mu\mu'}=\sqrt{2}(Z_{\mu s}\quad Z_{\mu r})\begin{pmatrix}\tau_{ss}&\tau_{sr}\\ \tau_{rs}&\tau_{rr}\end{pmatrix}\begin{pmatrix}X_{s\mu'}\\ X_{r\mu'}\end{pmatrix}. \tag{3.1}$$

The amplitudes connecting the (23) subsystem and the identical (12) or (13) subsystems are

$$\begin{pmatrix}X_{s\mu}\\ X_{r\mu}\end{pmatrix}=\sqrt{2}\begin{pmatrix}Z_{s\mu}\\ Z_{r\mu}\end{pmatrix}+\begin{pmatrix}Y_{ss}&Y_{sr}\\ Y_{rs}&Y_{rr}\end{pmatrix}\begin{pmatrix}\tau_{ss}&\tau_{sr}\\ \tau_{rs}&\tau_{rr}\end{pmatrix}\begin{pmatrix}X_{s\mu}\\ X_{r\mu}\end{pmatrix}, \tag{3.2}$$

and the common amplitudes in the identical (12) and (13) subsystems are

$$\begin{pmatrix}X_{ss}\\ X_{rs}\end{pmatrix}=\begin{pmatrix}Y_{ss}\\ Y_{rs}\end{pmatrix}+\begin{pmatrix}Y_{ss}&Y_{sr}\\ Y_{rs}&Y_{rr}\end{pmatrix}\begin{pmatrix}\tau_{ss}&\tau_{sr}\\ \tau_{rs}&\tau_{rr}\end{pmatrix}\begin{pmatrix}X_{ss}\\ X_{rs}\end{pmatrix}, \tag{3.3}$$

where the kernels $Y_{\sigma\sigma'}$ are defined by

$$Y_{\sigma\sigma'}=Z_{\sigma\sigma'}+\sqrt{2}(Z_{\sigma m}\quad Z_{\sigma n})\begin{pmatrix}\tau_{mm}&\tau_{mn}\\ \tau_{nm}&\tau_{nn}\end{pmatrix}\begin{pmatrix}Z_{m\sigma'}\\ Z_{n\sigma'}\end{pmatrix}. \tag{3.4}$$

In Eqs. (3.1)–(3.4), μ and μ' designate either m or n, the bound states in the (23) subsystem, and σ and σ' designate either s or r, where s designates the bound state in the (12) [or identical (13)] subsystem, and r is the resonance in that subsystem. The Z's are constructed from the form factors in the two-body finite-rank interactions, and the τ's are the two-body propagators. Detailed formulas for these are found in Ref. 20. The multiplications in these equations imply both the usual matrix multiplication, and an integral over one momentum vector variable (the **p** variable of Sec. II).

After angular-momentum reduction, (only S waves are used in both two- and three-body systems in this work) these equations become a set of coupled integral equations in one real variable, with singular kernels. They are solved by the Haftel-Tabakin[21] method, and the full S matrix, as a function of energy, is extracted. The S matrix is 1×1, 2×2, or 3×3, depending on how many channels are open in each of three energy sectors (elastic only, elastic plus one of inelastic or rearrangement, or all three, respectively). The program was tested in the work of Ref. 18, and the new additions to accommodate the resonance are merely direct extensions of that code. As well, internal consistency checks have been made, and finally the unitarity of the S matrix has been checked. Numerical stability of the results of the calculation has been established by varying the integration mesh sizes, and appropriate numbers of mesh points chosen. In the region of the resonance, the mesh has to be quite fine, to follow the rapid variations through the resonance. The code can have different numbers of mesh points in each of the three energy sectors.

Once the S matrix has been constructed, any physical observable can be calculated. For this work, what is needed is the time-delay matrix, $q_{\alpha\beta}(E)$, given by Eq. (2.26). For this, the calculated S matrix is fitted to a cubic spline, one spline for each S-matrix element as a function of energy. S and the derivative needed in Eq. (2.26) are calculated over a fine mesh of energies from the spline fit. The q matrix in Eq. (2.26) is diagonalized, and the eigenvalues and eigenvectors output. Some typical eigenvalues denoted here as $\Theta_n(E)$ as functions of the energy are shown in Fig. 1.

IV. TWO-BODY INTERACTIONS

Finite-rank separable interactions[22] simplify the two-body problem to solution of algebraic equations, and reduce the three-body problem to a set of coupled Lippmann-Schwinger-type equations in one vector variable.[20] Therefore, these are the type of interactions chosen for this study. The two-body interactions in both (distinct) two-body subsystems, (23) and (13), are rank-two interactions,

$$V_\alpha(q',q)=\sum_{n=1}^{2} g_{\alpha n}(q')\lambda_{\alpha n}g_{\alpha n}(q), \tag{4.1}$$

where α is the two-body channel index [1 for subsystem (23), 2 for subsystem (13)]. The interaction V_1 is exactly as in Ref. 18; that is,

$$g_{11}(q)=\frac{1}{q^2+\beta_1^2},\quad g_{12}(q)=\frac{1+\gamma_1 q^2}{(q^2+\beta_2^2)^2}. \tag{4.2}$$

The range parameters β_1 and β_2 have unrestricted values. The two binding energies $-\varepsilon_m$ and $-\varepsilon_n$ are also variable, but γ_1 is fixed by the constraint

$$\int_0^\infty \frac{g_{11}(q)g_{12}(q)}{q^2+\varepsilon_m}q^2dq=0. \tag{4.3}$$

This constraint is not essential in our formalism, but is imposed in order to simplify some of the expressions in the two-body problem. The strength parameters λ_{11} and λ_{12} are determined so as to give the chosen two-body binding energies.

The interaction V_2 is of the form discussed in Ref. 19; that is,

$$\begin{aligned} g_{21}(q)&=\frac{1}{q^2+\beta_3^2},\\ g_{22}(q)&=\frac{2\beta_4}{(q^2+\beta_4^2)^2}+2\gamma_2\frac{3\beta_4^2-q^2}{(q^2+\beta_4^2)^3}. \end{aligned} \tag{4.4}$$

Here the geometrical parameters β_3, β_4, and γ_2, and the binding energy ε_s are fixed arbitrarily, as well as the real part of the resonance energy E_r. The imaginary part of the resonance energy (the width Γ) is then fixed by

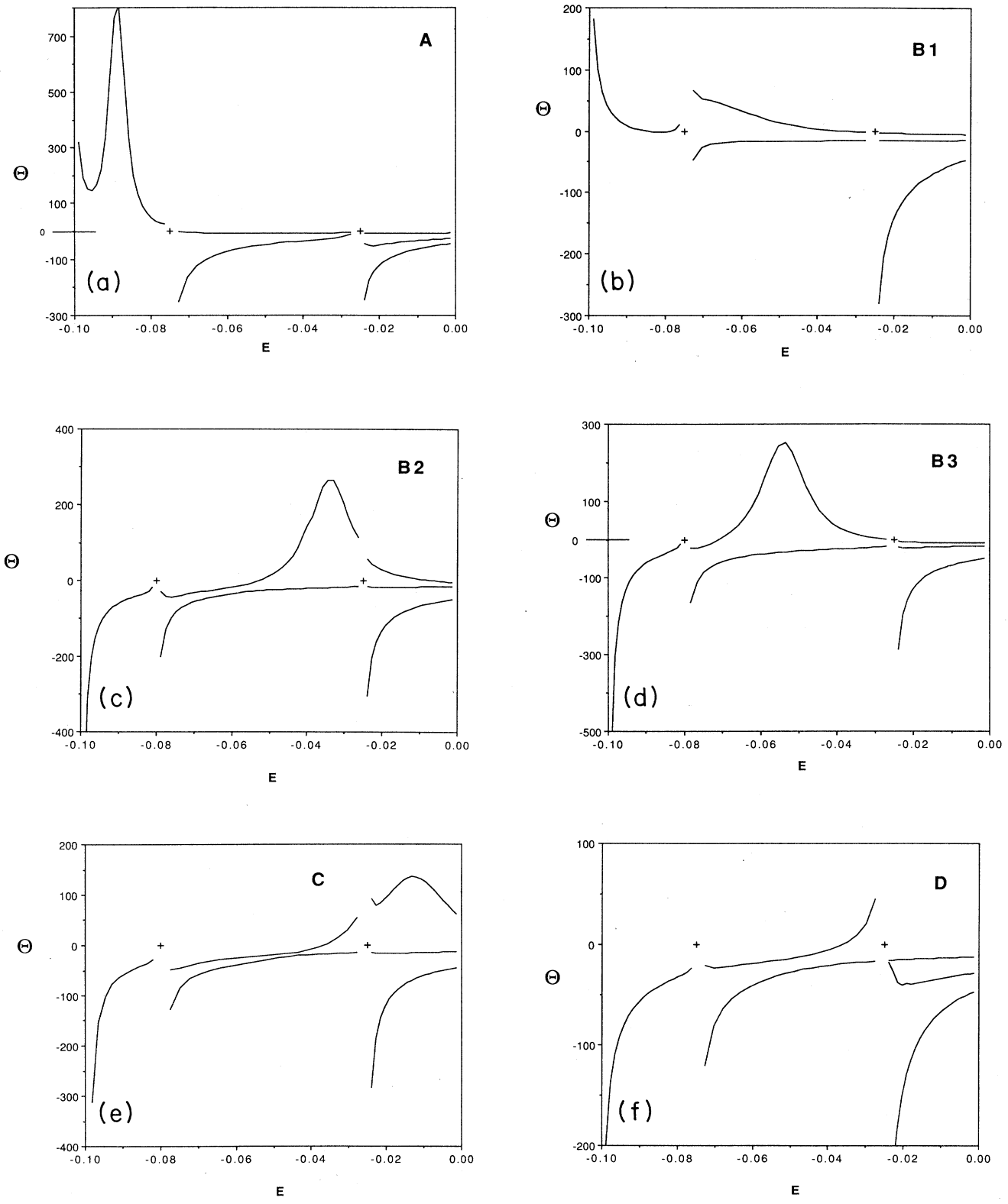

FIG. 1. Eigenvalues $\Theta_n(E)$ of the time-delay matrix for the selected cases. In all these figures, the E axis is in fm^{-2}, and the Θ is in inverse energy units (fm^2). (a) Case A, resonance in the elastic scattering sector. (b)–(d) Cases B, resonance in the second sector, where two channels are open. (e) and (f) Cases C and D, respectively. In case C, the resonance is in the energy sector where all three two-cluster channels are open. Case D is included for comparison, showing a "background" situation, where no resonance is observed below the breakup threshold.

demanding a zero in the Fredholm determinant at the complex energy

$$E=E_r-i\tfrac{1}{2}\Gamma \ . \tag{4.5}$$

It is not always possible to find such a solution. This limits the parameter space, defined by β_3, β_4, γ_2, ε_s, and E_r, of two-body interactions having both a bound state and a resonance. If the resonance is found, it may be either of the "weak" or "strong" variety, as discussed in Ref. 19. That is, the two-body phase shift may rise through $\pi/2$ at the resonance ("strong"), or it may rise, but not pass through $\pi/2$ ("weak"). Once the parameters, including Γ, are fixed in this way, the strengths λ_{21} and λ_{22} are determined.

In all the calculations reported in this work, we use the same two-body ground-state energy (hence elastic threshold) of $-\varepsilon_m=-0.10$ fm^{-2} (using $\hbar^2/m=41.43$ MeV fm^2, this corresponds to -4.14 MeV). Two versions of the interaction V_1 are used: one with energy $\varepsilon_n=0.075$ fm^{-2} (low inelastic threshold), the other with $\varepsilon_n=0.025$ fm^{-2} (high inelastic threshold). Likewise, the binding energy in the (13) subsystem, ε_s, has been taken at two values, $\varepsilon_s=0.025$ fm^{-2} (high rearrangement threshold), and $\varepsilon_s=0.080$ fm^{-2} (low rearrangement threshold). This way, we are able to reverse the order of the two thresholds. The real resonance energy E_r was varied over a range of values that gave a resonance condition, so as to put the resonance in each of the three energy sectors. A large number of different cases were attempted, but here we present only a few typical sample results.

Table I shows the parameter sets for which results are shown in the next section. The case A is one that has the resonance in the lowest energy sector that has only the elastic channel open. Cases $B1$ and $B2$ have the resonance in the second energy sector, where two channels are open, but with either order of the two thresholds. Case C has the resonance in the highest energy sector, where all three channels are open, and case D is, for comparison, one in which the resonance is so high as to be well above the breakup threshold. Case $B3$ is similar to $B2$, but is an example of a "weak" two-body resonance; that is, the two-body phase shift increases sharply at the energy of the resonance, but does not pass upward through $\pi/2$.

V. SAMPLE RESULTS

Calculations were carried out for a large variety of two-body potentials, which enabled the exploration of the possibilities that exist in this model. The selected cases (Table I) span the range of results obtained. In Fig. 1, we show graphs of the eigenvalues, $\Theta_n(E)$, of the time-delay matrix [Eq. (2.26)] as a function of energy from the elastic threshold to the breakup threshold, for each of the five cases. Here n ranges from 1 to the dimensionality of the S matrix. In all cases (except D, where the resonance energy E_r has deliberately been moved to a very high value) there is a peak in only one of the $\Theta_n(E)$ eigenvalues; namely, the highest one. (Note that a similar behavior of the time-delay eigenvalues has also been observed in Ref. 2.) This peak is positive, indicating a positive time delay, as would be expected from a resonant behavior. In most cases, the location of this peak is near where one would predict it on the basis of noninteracting cluster kinematics. Specifically, the resonant energy is E_r above the elastic threshold. Case $B1$, which is the most strongly damped one, shows the peak as a very broad structure, and shifted down considerably from where it might be expected. Generally, we have noticed in our results that the opening of the inelastic threshold appears to result in a very strong damping of the two-body resonance in the three-body system.

The plots of $\mathrm{tr}\, q_{\alpha i;\alpha i}(E)$ versus E carry a double physical meaning. First they display the total (in the sense of the trace) time delay versus energy. Second, because of the spectral property of the time delay [Eq. (2.28)], the same graph may be viewed as the state density shift as a function of the energy. In our sample calculations, we note that the general formula for state density shift is substantially simplified. We always have $E<0$, and since $\mathrm{Im}R_0(E+i0)=0$, the $R_0(z)$ portions may be deleted from $R_c(z)$; that is, there are no free three-body states with negative energy. In the elastic scattering sector,

TABLE I. Parameters of the two-body potentials used in this work. The units of the β's and γ_2 are fm^{-1}, γ_1 is in fm^2 and all the energies (ε's, E_r, and Γ) are in fm^{-2}.

		A	$B1$	$B2$	$B3$	C	D
V_1	β_1	0.25	0.25	1.444	1.444	1.444	0.25
	β_2	1.00	1.00	1.00	1.00	1.00	1.00
	γ_1	−3.8194	−3.8194	−1.7497	−1.7497	−1.7497	−3.8194
	ε_m	0.10	0.10	0.10	0.10	0.10	0.10
	ε_n	0.075	0.075	0.025	0.025	0.025	0.075
V_2	β_3	1.00	1.00	1.00	1.00	1.00	1.00
	β_4	1.01	1.01	1.01	1.01	1.01	1.01
	γ_2	−0.48	−0.48	−0.48	−0.48	−0.48	−0.48
	ε_s	0.025	0.025	0.080	0.080	0.080	0.025
	E_r	0.010	0.065	0.065	0.045	0.085	2.00
	Γ	0.001 416	0.011 856	0.000 027	0.000 480 "weak"	0.000 156	3.1569

there are further simplifications. Suppose H_α is the cluster Hamiltonian associated with the largest two-body binding energy. Then, the terms R_β, $\beta \neq \alpha$ do not contribute to the state density in the elastic energy sector, and so the state density shift reduces to

$$\mathrm{Tr}R_c(E+i0)=\mathrm{Tr}[R(E+i0)-R_\alpha(E+i0)] .$$

The curves of $\Theta_n(E)$ *versus* E indicate that, as anticipated, the time-delay matrix is indeed a useful characterization of resonant behavior. The positive delay is consistent with the intuitive notion of the scattered particle spending additional time in the neighborhood of the scattering region when resonating. This is in contrast with other, more traditional, methods of characterizing resonant behavior. For instance, neither the Argand diagram, nor the behavior of the phase shift in the region of the peak in $\Theta_n(E)$ show clearly identifiable behavior usually associated with resonances, in some of the cases studied here. Although the sample cases here, except $B3$, use only two-body resonances of the "strong" type, we note in passing that, as far as the time-delay matrix is concerned, there is no important distinction between the strong (e.g., $B2$) and weak (e.g., $B3$) resonances.

Next, let us elaborate on some of the ways used in phenomenological analysis of resonant behavior in the scattering process. The S matrix can be written in the form

$$S_{ij}=\eta_{ij}e^{2i\chi_{ij}} . \tag{5.1}$$

In this, the notation is changed from the general formulation in Eq. (2.19b). This is the energy-dependent reduced S matrix on the right-hand side of Eq. (2.19b), with the (ij) labels denoting the full description of whatever open channels are possible at this energy E. The labels i and j can have 1, 2, or 3 values, depending on which energy sector is under consideration. Because of unitarity, not all of the χ_{ij} and η_{ij} are independent. For S matrices of dimension 3 or less, only the diagonal χ_{ii} and η_{ii} are needed to determine the S matrix completely. Curves of these are shown in Fig. 2 for selected cases. In the first sector, only elastic scattering is possible, and the S matrix is 1×1, with $\eta_{11}=1$, and χ_{11} being the elastic phase shift. In the second sector, with two open channels, the S matrix is 2×2, and only one of the η_{ij} can be independently specified, and only two phase shifts, χ_{11} and χ_{22}. In the third sector, the S matrix is 3×3, and we need all three diagonal χ's and η's. We note in these figures that, generally, some "structure" is seen in the phase parameters in the neighborhood of the resonant behavior, but in most cases it is not of the type conventionally characterized as "resonant:" The phase shift does not generally pass *upward* through 90° at the resonance. In fact, the only case where such behavior shows up in the phase shift is case A, where the resonance is in the elastic sector. There the jump in the phase is almost exactly twice that in the two-body problem (Fig. 3), suggesting that the incoming particle resonates with each of the two target particles essentially independently of each other. The inelasticity parameters, η_{ii} indicate strong absorption in some cases, generally coinciding with strong damping of the resonance in the three-body system.

Cases $B1$ and $B2$ are similar, but with inversion of the two thresholds. In $B2$, the exchange threshold opens first, and the effect of the resonance is evident in phase χ_{11} (elastic channel) and in phase χ_{33} (exchange channel), unshifted with respect to the unperturbed position, as given by noninteracting cluster kinematics. In $B1$, the inelastic threshold is lower, and the effect of the resonance (evident in phase χ_{22} and coefficient η_{22}) seems to be damped and shifted downwards, with respect to the previous case. In both cases, the eigenphases (Fig. 4) have a smoother behavior, and do not cross. The effects of the resonance seem to be less evident in eigenphases.

The case C is an example of a resonance pushed above the second threshold. The effect of resonance is evident in phase shifts 1 and 3 and in the three coefficients η_{ii}. It is unshifted with respect to the unperturbed position, and this probably is related to the later opening of the inelastic channel.

Another traditional way of displaying resonant behavior, is the Argand diagram. From the elastic-scattering S-matrix element, S_{11}, we construct the T matrix,

$$S_{11}=1-2\pi i T_{11} , \tag{5.2}$$

and plot $\mathrm{Im}(T_{11})$ against $\mathrm{Re}(T_{11})$, see Fig. 5. Resonant behavior should show up as loops in the Argand diagram, but again, this is seen most strongly only in case A.

Our numerical results on the time-delay eigenvalues $\Theta_n(E)$, enable some comments to be made about threshold behavior. At threshold, a special mechanism is available to make time delay large (divergent) without having resonant behavior present. Recall that time delay is the difference between the transit times for the free evolution of incoming-outgoing clusters subtracted from the exact interacting transit time [Eq. (2.6) or (2.23)]. In the neighborhood of the threshold, cluster velocities may be very small. Thus, in this energy regime, both free and interacting transit times are typically divergent as the energy approaches threshold. Clearly, small percentage changes in the interacting and free cluster velocities will generally lead to an infinite time delay at threshold. It is evident that this is purely a kinematic effect and that no resonant behavior is taking place. Our computed examples for three-body scattering always show threshold singularities, and these singularities occur with both signs. Furthermore, threshold singularity divergences, like resonances, occur in only one eigenvalue of the time-delay matrix.

VI. CONCLUSIONS

The time-delay formalism is successful in exposing two-particle resonant behavior in what amounts to a complicated multiparticle scattering problem. The figures show the resonance manifest in a single eigenvalue of the q matrix. This behavior was already seen by Kupperman and Kaye,[2] for a one-dimensional chemical system. In this work we see such behavior in a three-dimensional three-body problem with a coupled-channel structure mimicking that typically encountered in nuclear reactions. We note that, away from thresholds, a

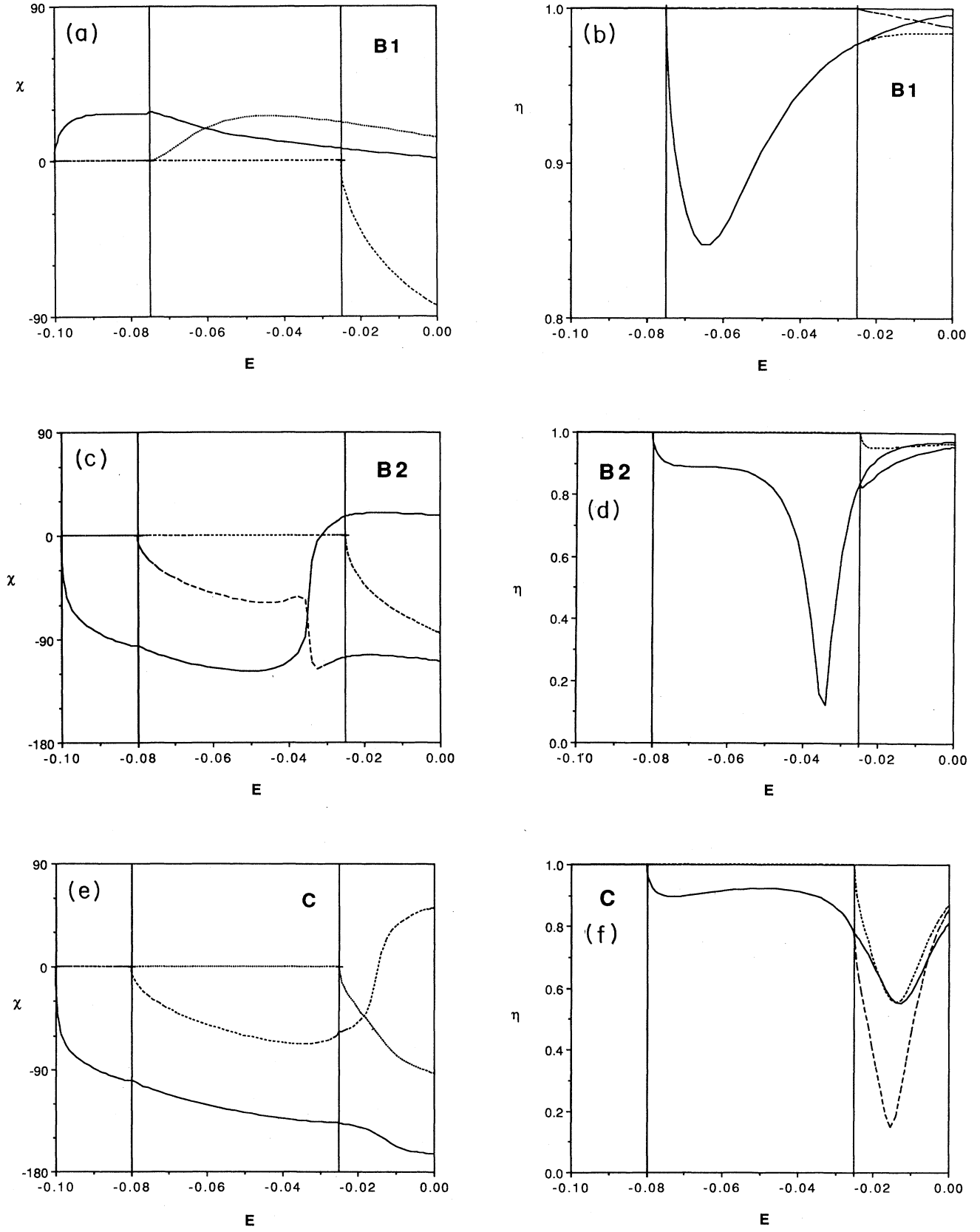

FIG. 2. Phase and inelasticity parameters [Eq. (5.1)] for a few selected cases: $B1$, $B2$, and C. In these figures, the solid line is the diagonal (11) element, the short-dashed one, the (22) element, and the long-dashed one the (33) element.

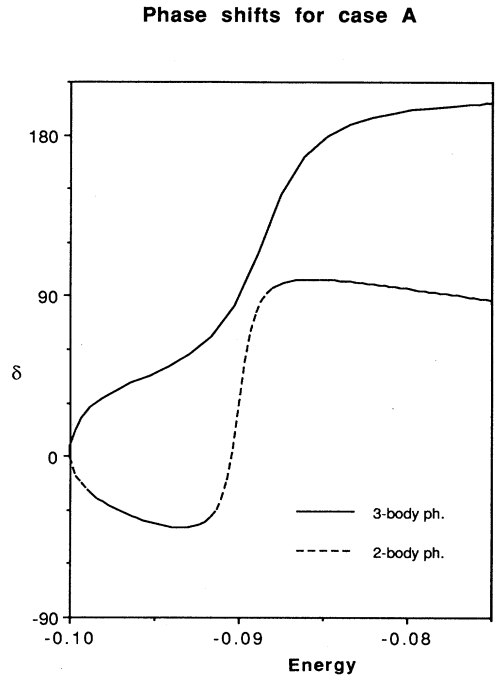

FIG. 3. Comparison of the two-body (dashed line) and three-body (solid line) phase shifts in case A, where the resonance is in the elastic sector.

large positive time-delay eigenvalue is a necessary condition and a unique signal identifying resonant behavior. A widely employed criterion for identifying resonant behavior is the requirement that the phase shift rise through $\pi/2$, with a jump in value of nearly π. In the three-body multichannel situation here, our results show that this criterion is not sufficiently general to describe all types of resonant behavior. This conclusion is in accord with the earlier observations of Dalitz and Moorhouse.[23]

In the case of many open channels, the eigenvalues of the q matrix are well separated in the neighborhood of the resonance "bump." This is in stark contrast to the general behavior of the phase shifts, which often appear to "cross" one another[24] resulting in a rapid variation of the phase (see, e.g., case $B2$ in Fig. 2). Since "crossing" does not occur for the eigenvalues of the q matrix, they are smoothly varying functions of the energy that provide a clear indication of resonance.

In an eigenphase analysis, many channels are affected by the resonance, thus making the resonance difficult to detect (Fig. 4). On the other hand, since the resonance affects only one eigenvalue of the q matrix, it is much easier to detect even very weak resonances. The distinction between eigenphases and the eigenvalues of the q matrix needs further clarification. While the q matrix contains the same information as the S matrix, in the eigenvalue analysis of these matrices, this information is presented in two distinct ways. An equation of the form (1.1) does not hold for the individual eigenphases. If the eigenphases of the S matrix are denoted $\Delta_n(E)$, the generalization of Eq. (1.1) is

$$\sum_n \Theta_n(E) = 2\sum_n \frac{d}{dE}\Delta_n(E) \ . \tag{6.1}$$

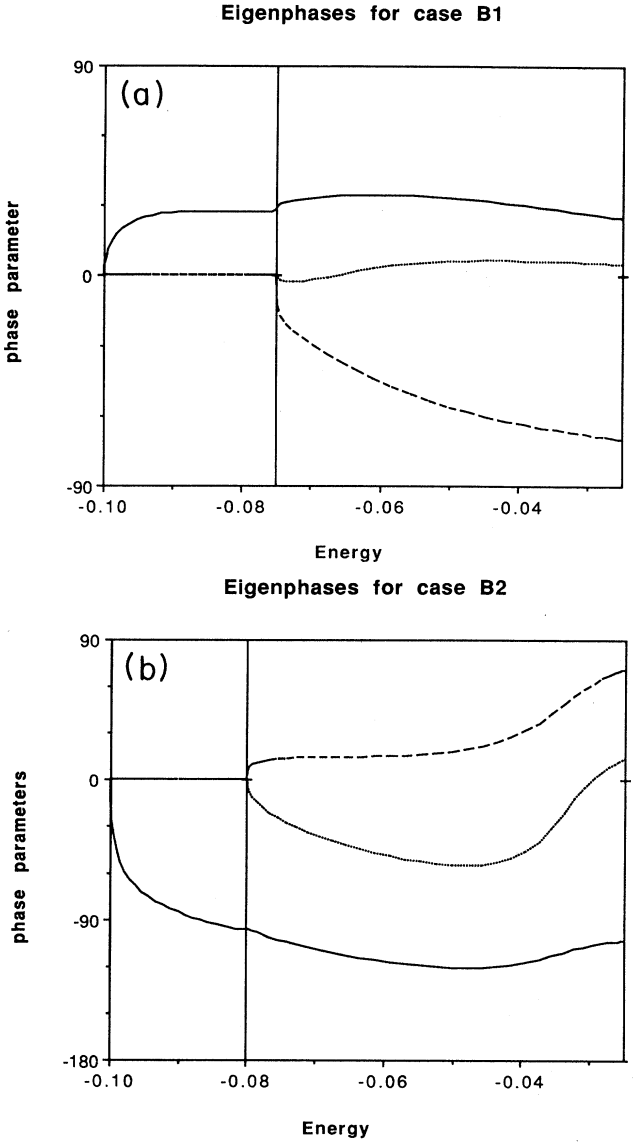

FIG. 4. Eigenphases and mixing coefficient for cases $B1$ and $B2$. Solid line is the eigenphase 1, short-dashed line eigenphase 2, and long-dashed line is the mixing coefficient.

This follows from the determinant exponentiation formula for matrices, and Eq. (2.26). Thus, while the resonance affects all the eigenphases $\Delta_n(E)$, the effect of the resonance can be isolated into a single one of the q-matrix eigenvalues $\Theta_n(E)$, as the simple Breit-Wigner form seen in Fig. 1. Extensive numerical investigations of the model (of which here we have shown only a few typical sample results) suggest that a resonance in the two-body subsystem will always affect only a single eigenvalue of the q matrix. Of course our result cannot give any indication of whether this would be true also of a three-body resonance that is not induced by an underlying two-body resonance mechanism. Nor does this simple model permit us to investigate what would happen in the presence of two resonances. The conjecture is that the two reso-

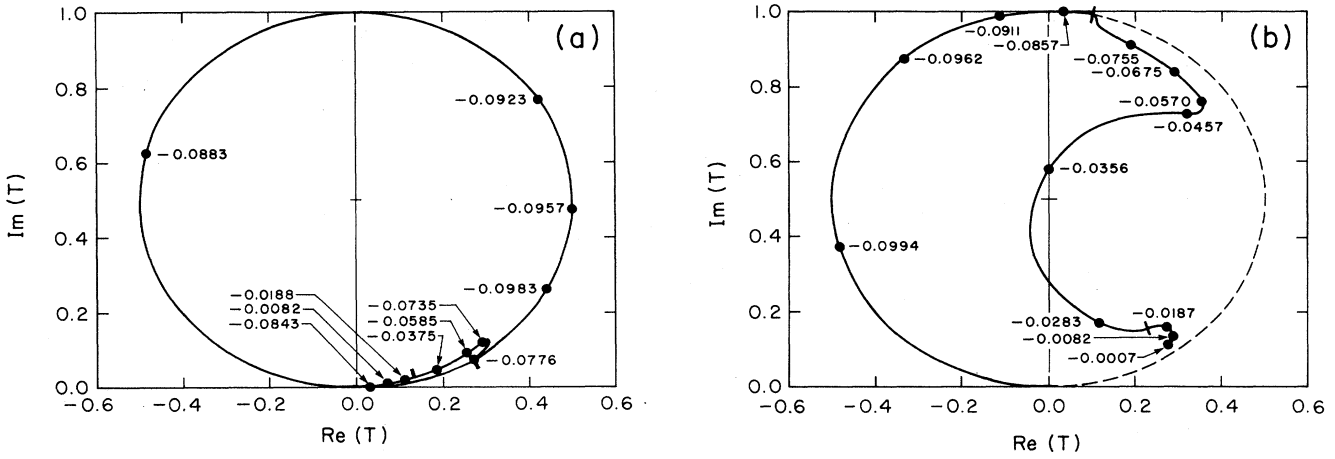

FIG. 5. Argand diagrams for cases A and $B2$. Some energy values (in fm^{-2}) are marked on the curves. The $\times$ marks the two thresholds. Note that in case A, the curve goes more than 360° around the unitary circle before the first threshold is reached.

nances would affect two different $\Theta_n(E)$, since these represent orthogonal degrees of freedom of the system.

ACKNOWLEDGMENTS

Part of this work was carried out while one of us (G.P.) was visiting the University of Manitoba and another of us (J.P.S.) visited the University of Padova. G. P. thanks the Department of Physics and the Research Board of the University of Manitoba for their hospitality and financial support. J. P. S. thanks the Department of Physics "Galileo Galilei" of the University of Padova for their hospitality and Istituto Nazionale di Fisica Nucleare (INFN) (Italy) for financial support. This work was supported in part by grants from the Natural Sciences and Engineering Research Council (NSERC) (Canada).

[1]E. Wigner, Phys. Rev. **98**, 145 (1955).
[2]A. Kupperman and J. A. Kaye, J. Phys. Chem. **85**, 1969 (1981).
[3]B. Simon, *Quantum Mechanics for Hamiltonians Defined as Quadratic Forms* (Princeton University Press, Princeton, N.J., 1971).
[4]S. Agmon, Ann. Scuola Norm. Sup. Pisa, Ser. IV 2, 151 (1975).
[5]T. A. Osborn and D. Bolle, J. Math Phys. **18**, 432 (1977).
[6]T. Dreyfus, Helv. Phys. Acta. **51**, 321 (1978).
[7]D. Bolle and T. A. Osborn, Phys. Rev. A **26**, 3062 (1982).
[8]F. T. Smith, J. Chem. Phys. **38**, 1304 (1963).
[9]R. Dashen and S. Ma, J. Math. Phys. **11**, 1136 (1970); **12**, 689 (1971).
[10]T. A. Osborn and T. Y. Tsang, Ann. Phys. (N.Y.) **101**, 119 (1976).
[11]D. Bolle, Ann. Phys. (N.Y.) **121**, 131 (1979).
[12]L. D. Faddeev, *Mathematical Aspects of the Three-Body Problem in Quantum Scattering Theory* (Daniel Davey, New York, 1965).
[13]F. T. Smith, Phys. Rev. **118**, 349 (1960).
[14]T. A. Osborn and D. Bolle, J. Math. Phys. **16**, 1533 (1975).
[15]D. Bolle and T. A. Osborn, J. Math. Phys. **20**, 1121 (1979).
[16]D. Wardlaw, P. Brummer, and T. A. Osborn, J. Chem. Phys. **76**, 4916 (1982).
[17]Ph. A. Martin, Acta Phys. Austriaca Suppl. **23**, 157 (1981).
[18]D. Eyre, T. A. Osborn, and J. P. Svenne, Phys. Rev. C **24**, 2409 (1981).
[19]G. Pisent and J. P. Svenne, Nuovo Cimento **97A**, 52 (1987).
[20]C. Lovelace, Phys. Rev. **135**, B1225 (1964); R. D. Amado, Annu. Rev. Nucl. Sci. **19**, 61 (1969).
[21]M. I. Haftel and F. Tabakin, Nucl. Phys. **A158**, 1 (1970).
[22]Y. Yamaguchi, Phys. Rev. **95**, 1628 (1954); Y. Yamaguchi and Y. Yamaguchi, *ibid.* **95**, 1635 (1954); F. Tabakin, Ann. Phys. (N.Y.) **30**, 51 (1964); L. Malthelitsch, W. Plessas, and W. Schweiger, Phys. Rev. **26**, 65 (1982); L. Beltramin, R. Del Frate, and G. Pisent, Nucl. Phys. **A442**, 266 (1985).
[23]R. H. Dalitz and R. G. Moorhouse, Proc. R. Soc. London, Ser. A **318**, 279 (1970).
[24]K. McVoy, in *Fundamentals in Nuclear Theory,* Lectures presented at an International Course, Trieste, 1966, edited by A. de-Shalit and C. Villi, (IAEA, Vienna, 1967) Chap. 8; C. J. Goebel and K. W. McVoy, Phys. Rev. **164**, 1932 (1967).